JOURNAL OF SOLID STATE CHEMISTRY **126,** 65–73 (1996)
ARTICLE NO. 0311

# Synthesis and Crystal Structure of $\sigma$-$Zn_{0.25}V_2O_5 \cdot H_2O$ with a Novel Type of $V_2O_5$ Layer[1]

Yoshio Oka,* Osamu Tamada,† Takeshi Yao,‡ and Naoichi Yamamoto†

*Department of Natural Environment Sciences, Faculty of Integrated Human Studies; †Graduate School of Human and Environmental Studies; and ‡Division of Energy and Hydrocarbon Chemistry, Graduate School of Engineering, Kyoto University, Kyoto 606, Japan

Received November 28, 1995; in revised form June 13, 1996; accepted June 17, 1996

**A new layered vanadium bronze designated as $\sigma$-phase $Zn_{0.25}V_2O_5 \cdot H_2O$ has been hydrothermally synthesized from $ZnCl_2$ and $VO(OH)_2$. A single-crystal study revealed the triclinic system $P\bar{1}$: $a = 10.614(2)$ Å, $b = 8.031(3)$ Å, $c = 10.7688(9)$ Å, $\alpha = 90.65(1)°$, $\beta = 91.14(1)°$, $\gamma = 90.09(2)°$, and $Z = 8$. The structure was solved and refined to $R/R_w = 0.079/0.048$ for 1580 reflections with $I > 3\sigma(I)$, which consists of $V_2O_5$ layers stacking along the $c$ axis and interstitial hydrated $Zn^{2+}$ ions. The $V_2O_5$ layer adopts a novel polyhedral framework built up of $VO_6$ octahedra, $VO_5$ trigonal bipyramids, and $VO_4$ tetrahedra. When projected parallel to the $ab$ plane, the $V_2O_5$ layer is described by the atomic sheet model in a manner similar to the $V_2O_5$ layer of $\delta$ phase such as $\delta$-$Ag_xV_2O_5$, that is, a double-sheet type composed of two $V_2O_5$ sheets facing each other. The interstitial Zn atom forms a $ZnO_6$ octahedron with two apical oxygens of the $VO_4$ tetrahedra on opposide sides and with four coplanar water molecules. The anhydrous $\sigma$ phase was obtained by heating the hydrate up to 200°C accompanied by the contraction in layer spacing from 10.76 to 8.92 Å.** 

## INTRODUCTION

Vanadium (IV, V) oxide bronzes $M_xV_nO_m$ often adopt layered structures consisting of $V_nO_m$ layers and interlayer $M$ ions that are sometimes in hydrous states. $V_nO_m$ layers so far known have compositions of $V_2O_5$, $V_3O_8$, and $V_4O_{11}$ of which a major group of the $M_xV_2O_5$ family has been extensively studied (1, 2). In the $M_xV_2O_5$ family there are two primary phases $\alpha$- and $\delta$-$M_xV_2O_5$, where to avoid complexity $\delta$-$M_xV_2O_5$ represents the related phases named $\varepsilon$-, $\rho$-, and $\nu$-$M_xV_2O_5$ as well. The $V_2O_5$ layers of the $\alpha$ and $\delta$ phases are structurally related to the oxide $V_2O_5$ (3) and $VO_2$(B) (4), respectively, and are also described by atomic sheet models as a single-sheet type for $\alpha$ phase and a double-sheet type for $\delta$ phase (5). Hagenmuller *et al.* (6, 7) studied $\alpha$ phases for a number of $M$ species and found rather narrow ranges of $x$ up to usually 0.03 and at most 0.11. They also reported an $\alpha'$ phase for $M$ = Na with $x = 0.7$ to 1.0 that is basically isomorphous to $\alpha$ phase (8). The structure of $\delta$ phase was first determined by Anderson (9) for $Ag_{0.68}V_2O_5$, and recently $\delta$ and related phases having double-sheet-type $V_2O_5$ layers were sorted and reviewed by Galy (10). Hydrated $\delta$ phases of $M_xV_2O_5 \cdot nH_2O$ were hydrothermally synthesized and structurally characterized by the present authors for $M$ = alkali metal ions (11, 12) and for $M = VO^{2+}$ (13). The values of $x$ for $\delta$ phase range more widely from 0.1 for $M = VO^{2+}$ (13) to 1.0 for $M = Cu^+$ (14). Besides the two phases $\gamma$-$LiV_2O_5$ has another type of $V_2O_5$ layer which may be grouped into a single-sheet type (15). It is of interest to add a new type of layer structure in the $M_xV_2O_5$ family. By using a hydrothermal method we have succeeded in synthesizing a new member of the $M_xV_2O_5$ family for $M$ = Zn formulated by a hydrous form $Zn_{0.25}V_2O_5 \cdot H_2O$. This new phase is named here as $\sigma$ phase. A single-crystal study revealed a novel structure of $V_2O_5$ layer with a double-sheet type. Comparisons of $\delta$ phase with $\delta$ phase for Zn compounds are also made.

## EXPERIMENTAL

### *Sample Preparation*

Hydrothermal synthesis was carried out in a $ZnCl_2$–$VO(OH)_2$ system, where $VO(OH)_2$ powders were prepared in advance hydrothermally at 150°C from a mixture of $VOSO_4$ and NaOH. A suspension of $VO(OH)_2$ powders in a 0.1 $M$ $ZnCl_2$ aqueous solution was sealed in a Pyrex ampoule and was treated in an autoclave at 280°C for 40 h. Products of shiny black powders were separated by filtra-

[1] See NAPS document No. 05329 for 54 pages of supplementary material. Order from ASIS/NAPS, Microfiche Publications, P.O. Box 3513, Grand Central Station, New York, NY 10163. Remit in advance $4.00 for microfiche copy or for photocopy, $7.75 for up to 20 pages plus $.30 for each additional page. All orders must be prepaid. Institutions and organizations may order by purchase order. However, there is a billing and handling charge for this service of $15. Foreign orders add $4.50 for postage and handling, for the first 20 pages, and $1.00 for each additional 10 pages of material, $1.50 for postage of any microfiche orders.



0022-4596/96 $18.00

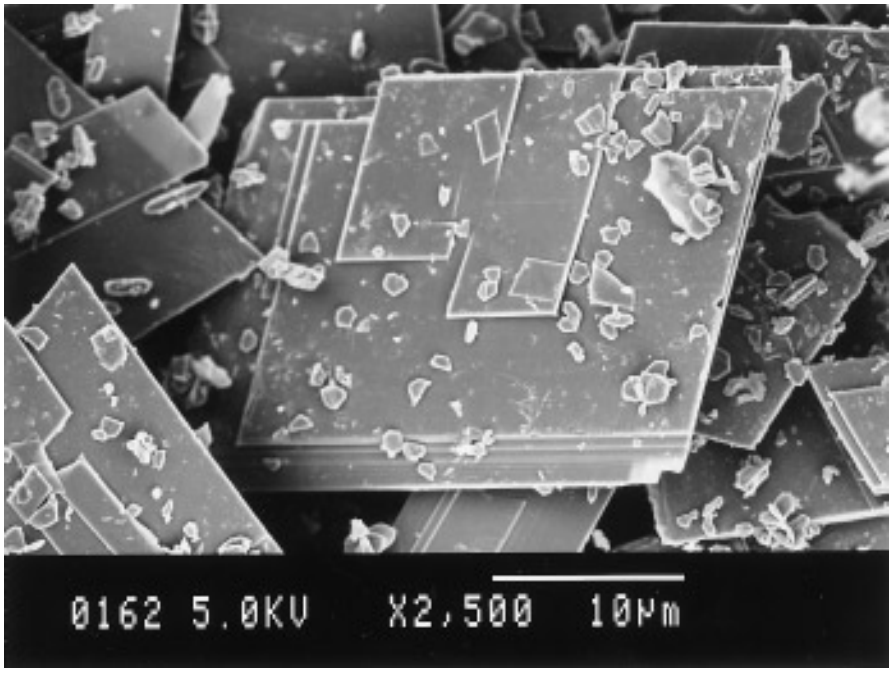


**FIG. 1.** Scanning electron micrograph of hydrothermally synthesized $\sigma$-$Zn_{0.25}V_2O_5 \cdot H_2O$ powders.

tion and washed thoroughly with distilled water. Powder X-ray diffractometry showed a highly oriented layered phase sometimes with small amounts of impurity phases of $VO_2$(A) and/or rutile-type $VO_2$. A chemical composition of the layered phase was determined to be $Zn_{0.25(1)}V_2O_5 \cdot nH_2O$ ($n \approx 1.0$) by an energy dispersive X-ray analysis, an atomic absorption analysis and a thermogravimetric analysis. As shown by the SEM picture in Fig. 1 the layered phase exhibits a flat rhombic shape. High-temperature X-ray diffraction measurements were carried out by using a Rigaku Rad-B system with monochromated CuK$\alpha$ radiation where a sample was heated by blowing hot air onto the surface to control temperature within $\pm 1$°C.

*Single-Crystal X-Ray Diffraction*

Single-crystal X-ray studies were performed on a crystal of dimensions $0.30 \times 0.08 \times 0.01$ mm. A preliminary study was made by using a Rigaku AFC-5S diffractometer and final data collection was made by using a Rigaku AFC-7R with higher intenstiy Mo$K\alpha$ radiation. The triclinic system was detected with lattice parameters of $a = 10.614(2)$ Å, $b = 8.031(3)$ Å, $c = 10.7688(9)$ Å, $\alpha = 90.65(1)°$, $\beta = 91.14(1)°$, and $\gamma = 90.09(1)°$ determined from 24 reflections in $20.4° \leq 2\theta \leq 27.4°$. Intensity data were collected up to $2\theta = 80°$ together with standard reflections of 5 3 0, $-5$ 3 0, and 5 $-3$ 0 which were monitored every 150 reflections to give no significant intensity fluctuation. An empirical correction of absorption effect was made using the $\psi$ scan method, resulting in transmission factors of 0.731–1.000. A total of 8734 unique reflections with $I > 0$ were obtained of which 1580 reflections with $I > 3\sigma(I)$ were used in the structure refinement. No more than 18% of total reflections were effective because of low signal-to-noise ratios of intensity profiles due to poor quality, thin shape, and tiny size of the crystal.

*Structure Determination*

The structure determination was performed by the Patterson and Fourier method using the program FRAXY (16). An initial model was derived based on the centrosymmetric space group $P\bar{1}$ and $Z = 8$. Preliminary structure refinements were executed using the program RADY (17). Atomic scattering factors for neutral atoms were taken from the ''International Tables for X-ray Crystallography IV'' (18). Sites of V atoms were successfully determined, which helped to locate oxygens and interlayer Zn atoms. Oxygens of interlayer water molecules denoted Ow were subsequently located in differential Fourier maps. The occupancies of interlayer Zn and Ow sites as well as V sites were checked to give no appreciable deviation from full occupancy and thus they were fixed to unity, yielding a stoichiometric composition $Zn_{0.25}V_2O_5 \cdot H_2O$. It is noted that isotropic temperature factors were solely used throughout the refinements owing to poor quality of the crystal and to a limited number of data for calculating the variables. The full-matrix least-square refinements led to $R/R_w = 0.079/0.048$ for 132 variables when the TEXSAN crystallographic software package (19) was used. The crys-

**TABLE 1**
**Crystallographic Data and Experimental Parameters for $\sigma$-$Zn_{0.25}V_2O_5 \cdot H_2O$**

| | |
|---|---|
| Chemical formula | $Zn_{0.25}V_2O_5 \cdot H_2O$ |
| Space group | $P\bar{1}$ |
| $a$ (Å) | 10.614(2) |
| $b$ (Å) | 8.031(3) |
| $c$ (Å) | 10.7688(9) |
| $\alpha$ (°) | 90.65(1) |
| $\beta$ (°) | 91.14(1) |
| $\gamma$ (°) | 90.09(2) |
| $Z$ | 8 |
| $D_c/gcm^{-3}$ | 3.130 |
| Crystal size (mm) | $0.30 \times 0.08 \times 0.01$ |
| Radiation | Mo$K\alpha$ |
| Scan technique | $2\theta - \omega$ |
| Scan width, $\Delta\omega$ (°) | $1.73 + 0.3\tan\theta$ |
| Scan speed $2\theta$ (° $min^{-1}$) | 16 |
| $2\theta_{max}$ (°) | 80 |
| No. unique reflections ($I > 0$) | 8734 |
| No. reflections ($I > 3\sigma(I)$) | 1580 |
| No. variables | 132 |
| $R$ | 0.079 |
| $R_w$ | 0.048 |

**TABLE 2**
**Atomic Parameters and Isotropic Temperature Factors for $\sigma$-$Zn_{0.25}V_2O_5 \cdot H_2O$**

| Atom | $x$ | $y$ | $z$ | $B_{eq}$ (Å$^2$) |
|---|---|---|---|---|
| V(1) | 0.7014(5) | 0.7187(6) | 0.1412(5) | 0.67(9) |
| V(2) | 0.6876(4) | 0.3407(6) | 0.1418(5) | 0.61(9) |
| V(3) | 0.9159(4) | 0.0412(6) | 0.1381(5) | 0.47(8) |
| V(4) | 0.4749(5) | 0.0340(6) | 0.1628(5) | 0.43(8) |
| V(5) | 0.2012(5) | 0.7859(6) | 0.1407(5) | 0.64(9) |
| V(6) | 0.1879(4) | 0.1623(6) | 0.1403(5) | 0.59(8) |
| V(7) | 0.4161(4) | 0.4632(6) | 0.1403(5) | 0.47(8) |
| V(8) | 0.9746(14) | 0.4701(6) | 0.1612(5) | 0.46(8) |
| Zn(1) | 0 | 1/2 | 1/2 | 1.51(8) |
| Zn(2) | 1/2 | 0 | 1/2 | 1.48(8) |
| O(1) | 0.814(2) | 0.522(2) | 0.124(2) | 0.3(3) |
| O(2) | 0.581(2) | 0.540(2) | 0.110(2) | 0.8(3) |
| O(3) | 0.790(2) | 0.194(2) | 0.080(2) | 1.0(3) |
| O(4) | 0.526(1) | 0.240(2) | 0.124(1) | 0.3(2) |
| O(5) | 0.831(2) | 0.868(2) | 0.087(2) | 1.0(3) |
| O(6) | 0.571(1) | 0.894(2) | 0.097(2) | 0.7(3) |
| O(7) | 0.311(2) | 0.986(2) | 0.124(2) | 0.3(3) |
| O(8) | 0.082(2) | 0.965(2) | 0.104(2) | 0.7(3) |
| O(9) | 0.289(2) | 0.310(2) | 0.078(2) | 0.9(3) |
| O(10) | 0.026(1) | 0.263(2) | 0.120(2) | 1.0(3) |
| O(11) | 0.332(2) | 0.635(2) | 0.089(2) | 1.1(3) |
| O(12) | 0.071(2) | 0.609(2) | 0.099(2) | 1.1(3) |
| O(13) | 0.706(2) | 0.738(2) | 0.289(2) | 1.4(4) |
| O(14) | 0.700(2) | 0.320(2) | 0.283(2) | 2.0(4) |
| O(15) | 0.904(2) | 0.042(2) | 0.286(2) | 1.5(4) |
| O(16) | 0.488(2) | 0.021(2) | 0.312(2) | 0.9(3) |
| O(17) | 0.205(2) | 0.768(2) | 0.290(2) | 1.6(4) |
| O(18) | 0.202(2) | 0.189(2) | 0.285(2) | 1.4(4) |
| O(19) | 0.404(2) | 0.465(2) | 0.286(2) | 1.0(3) |
| O(20) | 0.989(2) | 0.488(2) | 0.309(2) | 1.2(4) |
| Ow(1) | 0.032(2) | 0.759(3) | 0.495(2) | 3.5(5) |
| Ow(2) | 0.802(2) | 0.538(3) | 0.510(2) | 2.4(4) |
| Ow(3) | 0.516(3) | 0.264(3) | 0.507(3) | 4.4(6) |
| Ow(4) | 0.303(2) | 0.022(2) | 0.507(2) | 2.2(4) |

tallographic data and experimental parameters are listed in Table 1 and atomic parameters and isotropic temperature factors in Table 2.

## RESULTS AND DISCUSSION

### *Description of Crystal Structure*

As depicted in Fig. 2, a layered structure having a novel type of $V_2O_5$ layer has been disclosed which consists of V–O polyhedra of three kinds, namely, $VO_6$ octahedra for V(1), V(2), V(5), and V(6); $VO_5$ trigonal bipyramids for V(3) and V(7); and $VO_4$ tetrahedra for V(4) and V(8). We designate this novel phase as $\sigma$ phase or more specifically $\sigma$-$Zn_{0.25}V_2O_5 \cdot H_2O$ to differentiate from existing phases of, e.g., $\alpha$ and $\delta$. The bond distances and angles of the V–O polyhedra are listed in Table 3. It is indicated by the analysis of intensity data that the triclinic system can be approximated by the monoclinic system $P2_1/a$ when $\alpha$ and $\gamma$ parameters are set at 90°. Actually the extinction rule for $P2_1/a$ did not completely hold; some reflections of $0k0$ with $k = 2n + 1$ or $h0l$ with $h = 2n + 1$, for example, 010, 070, 100, and 102, showed weak but appreciable intensities. The triclinic system of this crystal is therefore said to be pseudo-monoclinic. In the monoclinic $P2_1/a$, atomic sites of $(x, y, z)$ and $(x + 1/2, 1/2 - y, z)$ are equivalent. This relationship is found to hold closely in following atomic pairs of the $V_2O_5$ layer: V(1)–V(5), V(2)–V(6), V(3)–V(7), V(4)–V(8), O(1)–O(7), O(2)–O(8), O(3)–O(9), O(4)–O(10), O(5)–O(11), O(6)–O(12), O(13)–O(17), O(14)–O(18), O(15)–O(19), and O(16)–O(20). For simplicity we describe the structure of $V_2O_5$ layer based on $P2_1/a$ by using the first atoms of each pair. The $V_2O_5$ layer now consists of V(1)$O_6$ and V(2)$O_6$ octahedra, V(3)$O_5$ trigonal bipyramid, and V(4)$O_4$ tetrahedron; V(1)$O_6$, V(2)$O_6$, V(3)$O_5$, and V(4)$O_4$ represent V(5)$O_6$, V(6)$O_6$, V(7)$O_5$, and V(8)$O_4$, respectively. In the *ab* plane, units of edge-sharing V(1)$O_6$–V(2)$O_6$–V(3)$O_5$ are connected to each other by sharing O(3) and O(5) vertices and are also joined through V(4)$O_4$ by sharing O(1), O(4), and O(6) vertices, forming a $V_2O_5$ sheet. Two $V_2O_5$ sheets are connected by sharing O(3)–O(5) edges between V(1)$O_6$ and V(2)$O_6$, making up a $V_2O_5$ layer. It should be useful to describe the structure of the $V_2O_5$ layer from another standpoint by utilizing an atomic sheet model as depicted in Fig. 3. A $V_2O_5$ sheet is composed of $VO_{1.5}$ and O sheets; V and O(1)–O(6) atoms at $z = 0.08$–$0.16$ are condensed into a

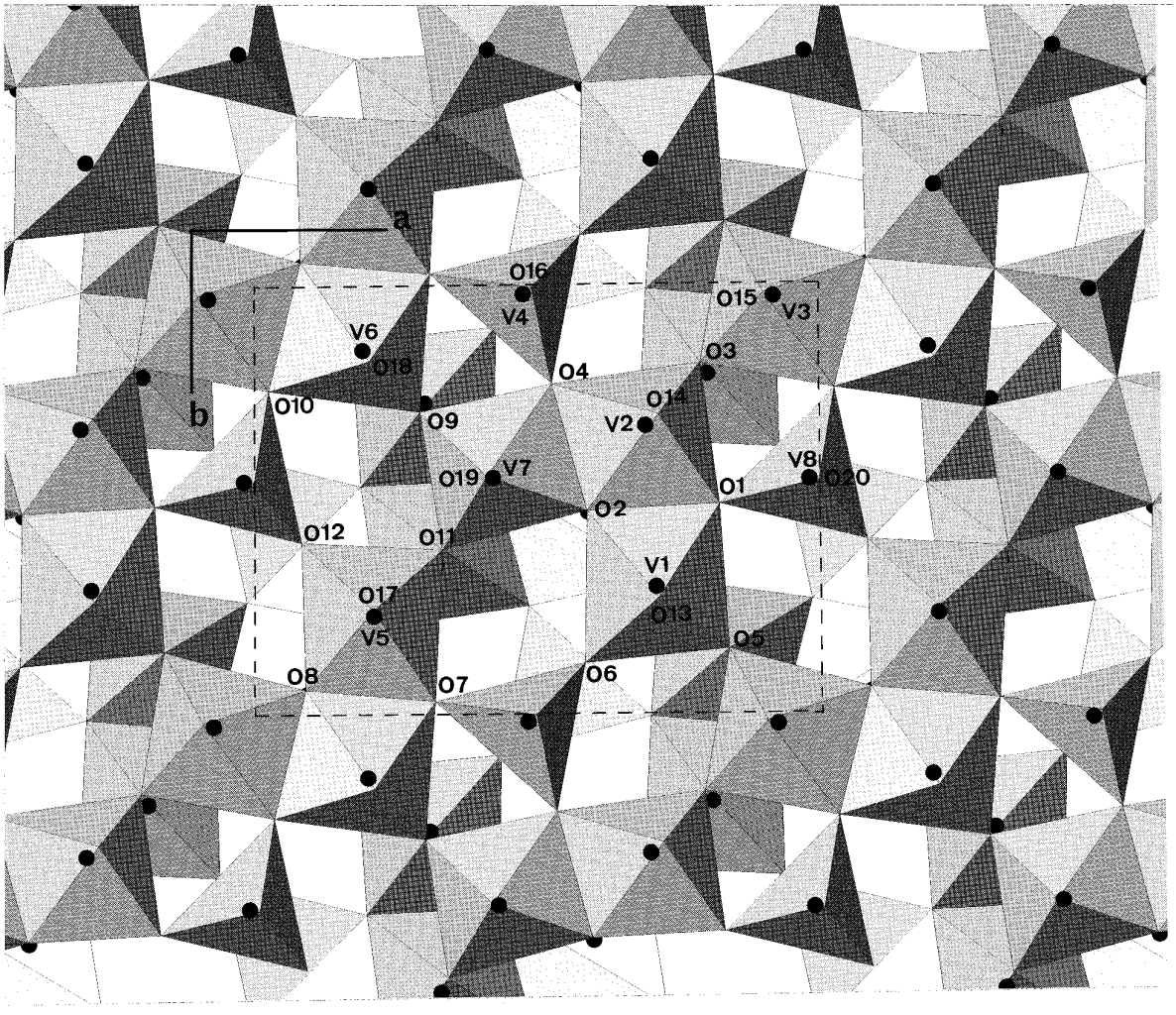


**FIG. 2.** Structure of $V_2O_5$ layer of $\sigma$-$Zn_{0.25}V_2O_5 \cdot H_2O$ projected onto the *ab* plane.

$VO_{1.5}$ sheet and O(13)–O(16) atoms at $z = 0.28$–$0.31$ into an O sheet. Two face-to-face $V_2O_5$ sheets are joined by V(1)–O(3) (actually V(1)–O(9) and V(5)–O(3) in Table 3) and V(2)–O(5) (actually V(2)–O(11) and V(6)–O(5) in Table 3) bonding to form a $V_2O_5$ layer. Consequently, the $V_2O_5$ layer of a $\sigma$ phase is regarded as a double-sheet type being analogous to the $V_2O_5$ layer of $\delta$ phase (12). It is interesting to make a comparison of $V_2O_5$ layer structures between $\sigma$ and $\delta$ phases as visualized in Fig. 4 for idealized *ab* planes of $V_2O_5$ sheets. The arrangement of V–O polyhedra of $\delta$ phase is that zigzag chains of edge-sharing $VO_6$ octahedra running along the *b* axis are connected by vertex sharing (Fig. 4b) while that of $\sigma$ phase is that edge-sharing triads and tetrahedra are connected by vertex sharing (Fig. 4a). As expected from the structural relation of the *ab* plane between both phases, the area of the *ab* plane for $\sigma$ phase (85.64 Å$^2$) is close to twice that of $\delta$ phase (42.6–43.8 Å$^2$).

An interlayer Zn atom is octahedrally coordinated, as depicted in Fig. 5, by two apical oxygens of $V(4)O_4$ on opposite sides and by four coplanar water molecules with bond distances and angles listed in Table 4. Since Z(1) and Z(2) are located in equivalent positions of $P2_1/a$, $Zn(1)O_6$ and $Zn(2)O_6$ octahedra are reduced to one $ZnO_6$ of Zn–(O(16) × 2, Ow(1) × 2, Ow(2) × 2) under $P2_1/a$. It should be noted that Zn atom is placed in the position right above and below the apical O(16) atoms, which seems to determine the relative locations of adjacent $V_2O_5$ layers. The apical O(16) atom is attracted by an Zn atom, resulting in a larger $z$ parameter ($z = 0.31$) than those ($z = 0.28$ – 29) of other apical oxygens. Concomitantly the tetrahedral V(4) atom also exhibits a $z$ parameter ($z = 0.16$) larger than those ($z = 0.14$) of other V atoms. The values of $x$ and $n$ in $Zn_xV_2O_5 \cdot nH_2O$ must not exceed 0.25 and 1.0, respectively, yielding a limited composition of $Zn_{0.25}V_2O_5 \cdot H_2O$.

## TABLE 3
## Bond Distances (Å) and Angles (°) for V–O Polyhedra

$V(1)O_6$ octahedron

| | | | | | |
|---|---|---|---|---|---|
| V(1)–O(1) | 2.00(2) | V(1)–O(2) | 1.94(2) | V(1)–O(5) | 1.92(2) |
| V(1)–O(6) | 2.03(2) | V(1)–O(13) | 1.59(2) | V(1)–O(9)$^a$ | 2.37(2) |
| O(1)–V(1)–O(2) | | 78.0(7) | O(1)–V(1)–O(5) | | 91.7(7) |
| O(1)–V(1)–O(6) | | 159.7(7) | O(1)–V(1)–O(13) | | 98.8(9) |
| O(1)–V(1)–O(9)$^a$ | | 78.6(7) | O(2)–V(1)–O(5) | | 151.2(7) |
| O(2)–V(1)–O(6) | | 91.8(7) | O(2)–V(1)–O(13) | | 104.2(9) |
| O(2)–V(1)–O(9)$^a$ | | 78.9(7) | O(5)–V(1)–O(6) | | 89.0(7) |
| O(5)–V(1)–O(13) | | 104.0(9) | O(5)–V(1)–O(9)$^a$ | | 72.7(7) |
| O(6)–V(1)–O(13) | | 100.6(9) | O(6)–V(1)–O(9)$^a$ | | 82.3(6) |
| O(13)–V(1)–O(9)$^a$ | | 175.6(9) | | | |

$V(2)O_6$ octahedron

| | | | | | |
|---|---|---|---|---|---|
| V(2)–O(1) | 1.99(2) | V(2)–O(2) | 1.99(2) | V(2)–O(3) | 1.74(2) |
| V(2)–O(4) | 1.90(1) | V(2)–O(14) | 1.54(2) | V(2)–O(11)$^a$ | 2.50(2) |
| O(1)–V(2)–O(2) | | 77.1(7) | O(1)–V(2)–O(3) | | 91.5(8) |
| O(1)–V(2)–O(4) | | 155.4(7) | O(1)–V(2)–O(14) | | 98.0(9) |
| O(1)–V(2)–O(11)$^a$ | | 83.2(6) | O(2)–V(2)–O(3) | | 146.5(8) |
| O(2)–V(2)–O(4) | | 79.4(7) | O(2)–V(2)–O(14) | | 108(1) |
| O(2)–V(2)–O(11)$^a$ | | 73.6(7) | O(3)–V(2)–O(4) | | 104.3(7) |
| O(3)–V(2)–O(14) | | 105(1) | O(3)–V(2)–O(11)$^a$ | | 73.8(7) |
| O(4)–V(2)–O(14) | | 96.1(9) | O(4)–V(2)–O(11)$^a$ | | 83.2(6) |
| O(14)–V(2)–O(11)$^a$ | | 178.2(9) | | | |

$V(3)O_5$ trigonal bipyramid

| | | | | | |
|---|---|---|---|---|---|
| V(3)–O(3) | 1.92(2) | V(3)–O(5)$^b$ | 1.75(2) | V(3)–O(8)$^c$ | 1.91(2) |
| V(3)–O(10)$^d$ | 2.14(2) | V(3)–O(15) | 1.60(2) | | |
| O(3)–V(3)–O(5)$^b$ | | 93.2(8) | O(3)–V(3)–O(8)$^c$ | | 72.4(7) |
| O(3)–V(3)–O(10)$^d$ | | 79.1(7) | O(3)–V(3)–O(15) | | 105.3(9) |
| O(5)$^b$–V(3)–O(8)$^c$ | | 72.1(7) | O(5)$^b$–V(3)–O(10)$^d$ | | 156.3(8) |
| O(5)$^b$–V(3)–O(15) | | 105.0(9) | O(8)$^c$–V(3)–O(10)$^d$ | | 84.3(6) |
| O(8)$^c$–V(3)–O(15) | | 175.9(8) | O(10)$^d$–V(3)–O(15) | | 98.7(8) |

$V(4)O_4$ tetrahedron

| | | | | | |
|---|---|---|---|---|---|
| V(4)–O(4) | 1.80(1) | V(4)–O(6)$^b$ | 1.68(2) | V(4)–O(7)$^b$ | 1.82(2) |
| V(4)–O(16) | 1.62(2) | | | | |
| O(4)–V(4)–O(6)$^b$ | | 109.2(8) | O(4)–V(4)–O(7)$^b$ | | 115.5(7) |
| O(4)–V(4)–O(16) | | 106.3(8) | O(6)$^b$–V(4)–O(7)$^b$ | | 110.3(8) |
| O(6)$^b$–V(4)–O(16) | | 109.2(9) | O(7)$^b$–V(4)–O(16) | | 106.2(9) |

$V(5)O_6$ octahedron

| | | | | | |
|---|---|---|---|---|---|
| V(5)–O(7) | 1.99(2) | V(5)–O(8) | 1.95(2) | V(5)–O(11) | 1.94(2) |
| V(5)–O(12) | 2.03(2) | V(5)–O(17) | 1.62(2) | V(5)–O(3)$^a$ | 2.39(2) |
| O(7)–V(5)–O(8) | | 76.5(7) | O(7)–V(5)–O(11) | | 92.9(7) |
| O(7)–V(5)–O(12) | | 160.2(7) | O(7)–V(5)–O(17) | | 99.6(9) |
| O(7)–V(5)–O(3)$^a$ | | 79.0(7) | O(8)–V(5)–O(11) | | 150.6(7) |
| O(8)–V(5)–O(12) | | 91.9(7) | O(8)–V(5)–O(17) | | 106(1) |
| O(8)–V(5)–O(3)$^a$ | | 77.3(7) | O(11)–V(5)–O(12) | | 89.5(7) |
| O(11)–V(5)–O(17) | | 102.6(9) | O(11)–V(5)–O(3)$^a$ | | 73.8(7) |
| O(12)–V(5)–O(17) | | 99.0(9) | O(12)–V(5)–O(3)$^a$ | | 82.9(6) |
| O(17)–V(5)–O(3)$^a$ | | 176.0(9) | | | |

$V(6)O_6$ octahedron

| | | | | | |
|---|---|---|---|---|---|
| V(6)–O(7)$^b$ | 1.94(2) | V(6)–O(8)$^b$ | 1.98(2) | V(6)–O(9) | 1.74(2) |
| V(6)–O(10) | 1.92(2) | V(6)–O(18) | 1.57(2) | V(6)–O(5)$^a$ | 2.46(2) |
| O(7)$^b$–V(6)–O(8)$^b$ | | 77.2(7) | O(7)$^b$–V(6)–O(9) | | 92.6(8) |
| O(7)$^b$–V(6)–O(10) | | 155.2(7) | O(7)$^b$–V(6)–O(18) | | 97.5(9) |
| O(7)$^b$–V(6)–O(5)$^a$ | | 83.6(7) | O(8)$^b$–V(6)–O(9) | | 145.3(8) |
| O(8)$^b$–V(6)–O(10) | | 79.1(7) | O(8)$^b$–V(6)–O(18) | | 109.6(9) |
| O(8)$^b$–V(6)–O(5)$^a$ | | 72.7(7) | O(9)–V(6)–O(10) | | 102.9(8) |
| O(9)–V(6)–O(18) | | 104(1) | O(9)–V(6)–O(5)$^a$ | | 73.3(7) |
| O(10)–V(6)–O(18) | | 97.3(9) | O(10)–V(6)–O(5)$^a$ | | 82.5(6) |
| O(18)–V(6)–O(5)$^a$ | | 177.5(8) | | | |

$V(7)O_5$ trigonal bipyramid

| | | | | | |
|---|---|---|---|---|---|
| V(7)–O(9) | 1.93(2) | V(7)–O(11)$^d$ | 1.73(2) | V(7)–O(2) | 1.89(2) |
| V(7)–O(4) | 2.14(2) | V(7)–O(19) | 1.58(2) | | |
| O(9)–V(7)–O(11)$^d$ | | 92.5(7) | O(9)–V(7)–O(2) | | 71.1(6) |
| O(9)–V(7)–O(4) | | 79.7(6) | O(9)–V(7)–O(19) | | 105.9(9) |
| O(11)–V(7)–O(2) | | 72.2(7) | O(11)–V(7)–O(4) | | 156.9(7) |
| O(11)–V(7)–O(19) | | 105.6(9) | O(2)–V(7)–O(4) | | 84.6(6) |
| O(2)–V(7)–O(19) | | 176.0(8) | O(4)–V(7)–O(19) | | 97.5(8) |

$V(8)O_4$ tetrahedron

| | | | | | |
|---|---|---|---|---|---|
| V(8)–O(10)$^d$ | 1.80(2) | V(8)–O(12)$^d$ | 1.66(2) | V(8)–O(1) | 1.79(2) |
| V(8)–O(20) | 1.60(2) | | | | |
| O(10)$^d$–V(8)–O(12)$^d$ | | 109.4(8) | O(10)$^d$–V(8)–O(1) | | 116.7(7) |
| O(10)$^d$–V(8)–O(20) | | 107.0(9) | O(12)$^d$–V(8)–O(1) | | 109.8(8) |
| O(12)$^d$—V(8)–O(20) | | 107.5(9) | O(1)–V(8)–O(20) | | 105.9(9) |

*Note.* Symmetry codes: $^a$ $1 - x, 1 - y, -z$; $^b$ $x, y - 1, z$; $^c$ $x, y - 1, 1 + z$; $^d$ $1 + x, y, z$.

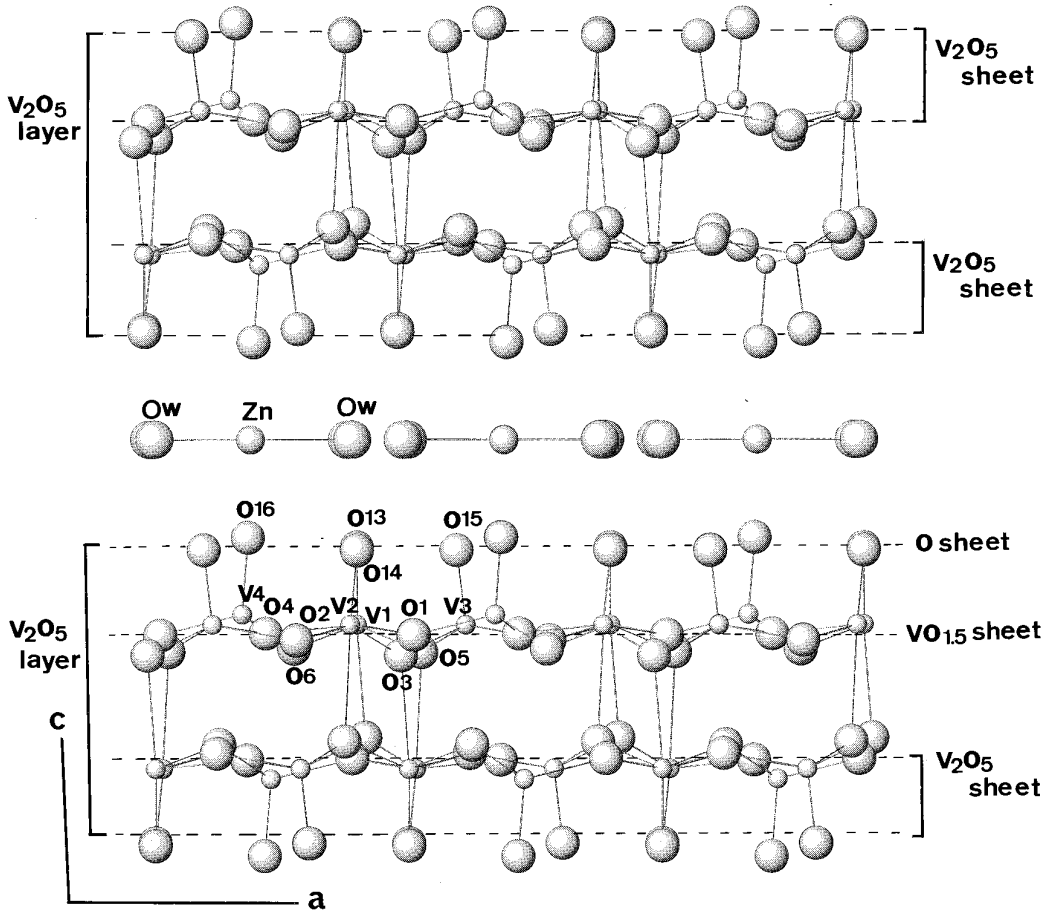


**FIG. 3.** Representation for double-sheet-type $V_2O_5$ layers for $\sigma$-$Zn_{0.25}V_2O_5 \cdot H_2O$ viewed along the *b* axis.

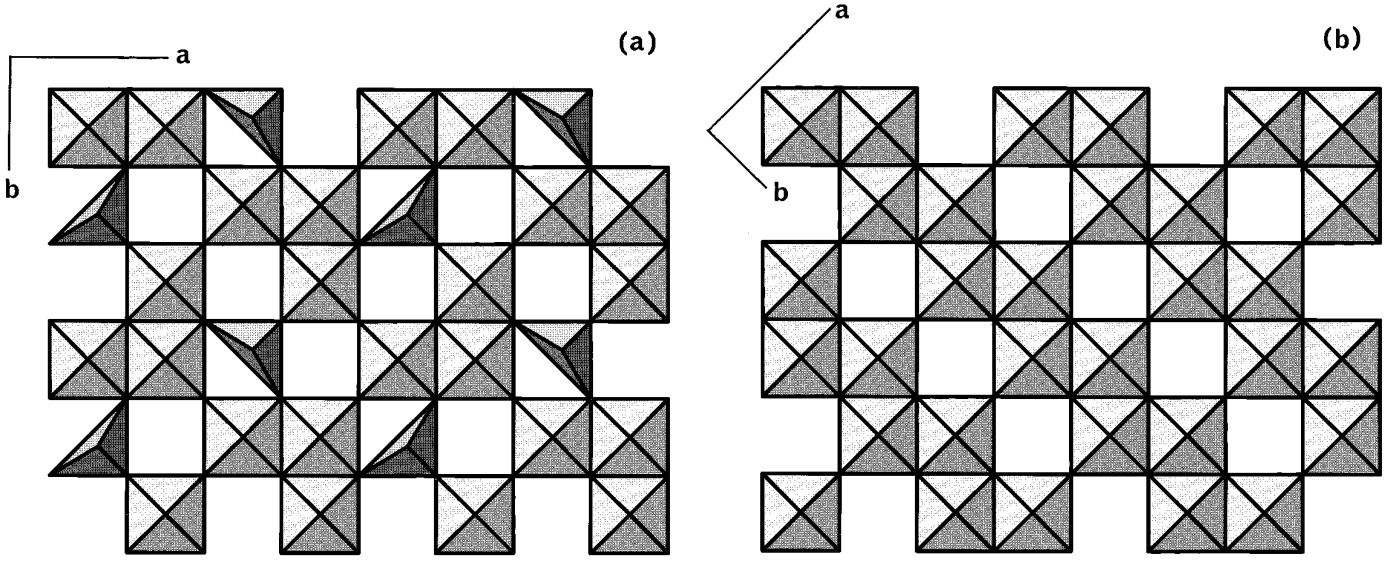


**FIG. 4.** Polyhedral representations for idealized structures of $V_2O_5$ sheet in the *ab* plane for (a) $\sigma$ phase and (b) $\delta$ phase.

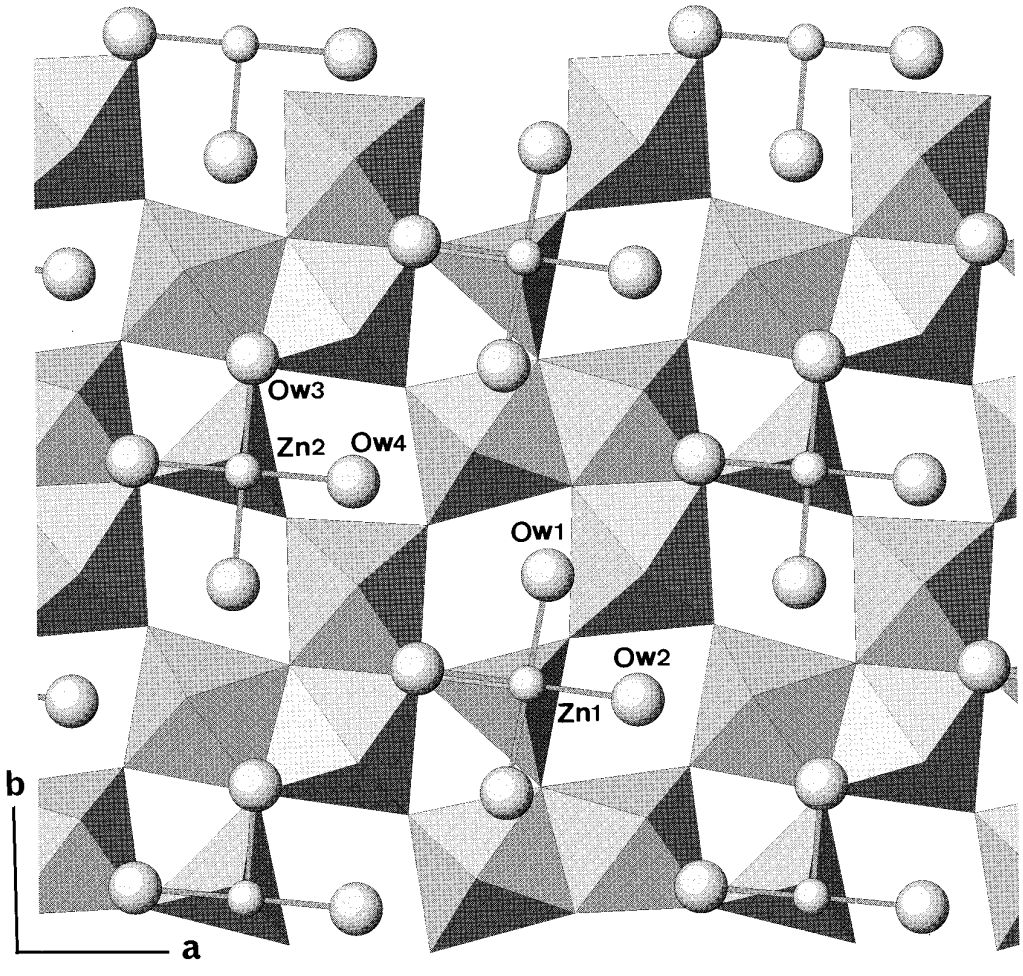


**FIG. 5.** Locations of interstitial Zn atoms and water molecules in a interlayer region between $V_2O_5$ layers. Zn atoms and water molecules are denoted by small and large circles, respectively, and a $V_2O_5$ layer is indicated by a polyhedral representation of a $V_2O_5$ sheet.

*Lattice Distortion into Triclinic System*

The structure of $\sigma$-phase structure is well described based on the monoclinic $P2_1/a$ but actually adopts the triclinic system. As described above, the positions of V and O atoms in the $V_2O_5$ layer as well as interlayer Zn atoms show the approximate relation of $(x, y, z)$–$(x + 1/2, 1/2 - y, z)$ derived from the symmetry operation of $P2_1/a$. However as can be seen from Table 4, the relation is not applied to the positions of interlayer water molecules. Instead, the approximate relation of $(x, y, z)$–$(x + 1/2, y + 1/2, z)$ is found for Ow(1)–Ow(3) and Ow(2)–Ow(4), which corresponds to the C-type lattice or consistent with the positional relation of Zn atoms. Therefore interlayer water molecules possibly cause the lattice distortion from monoclinic to triclinic. Figure 6 visualizes the locations of water molecules for the $P2_1/a$ symmetry in comparison with the C-type symmetry, where Ow(1)–Ow(3′) and Ow(2)–Ow(4′) have the $(x, y, z)$–$(x + 1/2, 1/2 - y, z)$ of $P2_1/a$. It is quite likely that $P2_1/a$ is realized when Ow(3) and Ow(4) are replaced by Ow(3′) and Ow(4′), respectively.

*Phase Change into Anhydrous $\sigma$ Phase*

Hydrated $\sigma$-$Zn_{0.25}V_2O_5 \cdot H_2O$ was converted into anhydrous $\sigma$-$Zn_{0.25}V_2O_5$ by heating as demonstrated by the TG-DTA diagram in Fig. 7. At a heating rate of 5°C $min^{-1}$ dehydration gradually proceeded above 70°C, developed rapidly around 170°C, and finished around 200°C accompanied by a broad endothermic DTA peak. The anhydrous phase was examined by high-temperature X-ray diffraction, and the pattern at 200°C is presented together with the pattern at RT in Fig. 8. The layer spacing was found to contract from 10.76 to 8.92 Å by dehydration. In the anhydrous phase Zn atoms must shift to an appropriate site which is coordinated by more apical oxygens than in the hydrated phase. The structural details of the anhydrous phase, however, remain unknown.

**TABLE 4**
**Bond Distances (Å) and Angles (°) for Zn–O Octahedra**

| | | | |
|---|---|---|---|
| | $Zn(1)O_6$ octahedron | | |
| Zn(1)–Ow(1)[a,b] | 2.11(2) | Zn(1)–Ow(2)[c,d] | 2.13(2) |
| Zn(1)–O(20)[c,d] | 2.06(2) | | |
| Ow(1)[a]–Zn(1)Ow(1)[b] | 180.0(1) | Ow(1)[a]–Zn(1)–Ow(2)[c] | 88.8(8) |
| Ow(1)[a]–Zn(1)Ow(2)[b] | 91.2(8) | Ow(1)[a]–Zn(1)–O(20)[c] | 90.9(8) |
| Ow(1)[a]–Zn(1)O(20)[d] | 89.1(8) | Ow(1)[b]–Zn(1)–Ow(2)[c] | 91.2(8) |
| Ow(1)[b]–Zn(1)Ow(2)[d] | 88.8(8) | Ow(1)[b]–Zn(1)–O(20)[c] | 89.1(8) |
| Ow(1)[b]–Zn(1)O(20)[d] | 90.9(8) | Ow(2)[c]–Zn(1)–Ow(2)[d] | 180.0(1) |
| Ow(2)[c]–Zn(1)O(20)[c] | 89.0(9) | Ow(2)[c]–Zn(1)–O(20)[d] | 89.0(9) |
| Ow(2)[d]–Zn(1)O(20)[c] | 89.0(9) | Ow(2)[d]–Zn(1)–O(20)[d] | 91.0(9) |
| O(20)[c]–Zn(1)O(20)[d] | 180.0(1) | | |
| | $Zn(2)O_6$ octahedron | | |
| Zn(2)–Ow(3)[a,e] | 2.12(2) | Zn(2)–Ow(4)[a,e] | 2.11(2) |
| Zn(2)–O(16)[a,e] | 2.03(2) | | |
| Ow(3)[a]–Zn(2)Ow(3)[e] | 180.0(1) | Ow(3)[a]–Zn(2)–Ow(4)[e] | 89.6(8) |
| Ow(3)[a]–Zn(2)Ow(4)[e] | 90.4(8) | Ow(3)[a]–Zn(2)–O(16)[a] | 93.0(9) |
| Ow(3)[a]–Zn(2)O(16)[e] | 87.0(9) | Ow(3)[e]–Zn(2)–Ow(4)[a] | 90.4(8) |
| Ow(3)[e]–Zn(2)Ow(4)[e] | 89.6(8) | Ow(3)[e]–Zn(2)–O(16)[a] | 87.0(9) |
| Ow(3)[e]–Zn(2)O(16)[e] | 93.0(9) | Ow(4)[a]–Zn(2)–Ow(4)[e] | 180.0(1) |
| Ow(4)[a]–Zn(2)O(16)[a] | 90.9(8) | Ow(4)[a]–Zn(2)–O(16)[e] | 89.1(8) |
| Ow(4)[e]–Zn(2)O(16)[a] | 89.1(8) | Ow(4)[e]–Zn(2)–O(16)[e] | 90.9(8) |
| O(16)[a]–Zn(2)O(16)[e] | 180.0(1) | | |

*Note.* Symmetry codes: [a] $x, y, z$; [b] $-x, 1-y, 1-z$; [c] $1-x, 1-y, 1-z$; [d] $x-1, y, z$; [e] $1-x, -y, 1-z$.

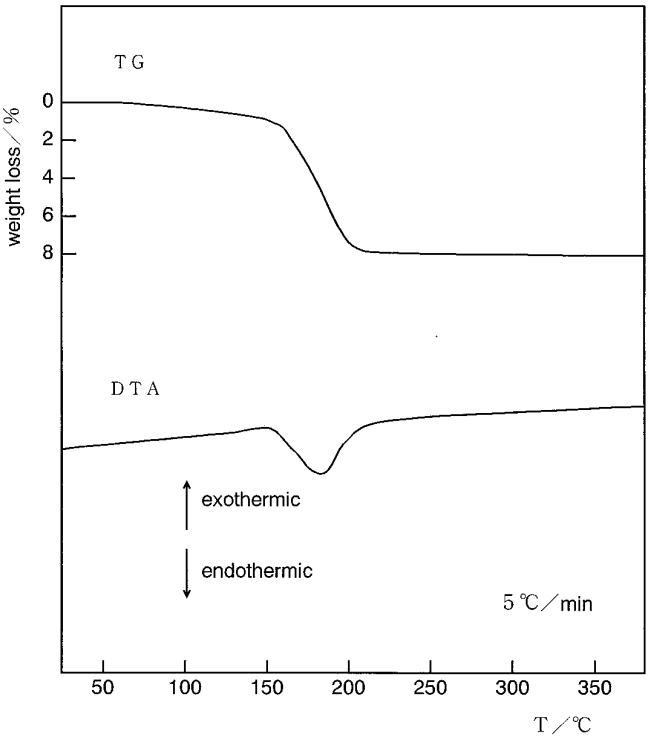


**FIG. 7.** TG-DTA diagram for $\sigma$-$Zn_{0.25}V_2O_5 \cdot H_2O$ recorded at a heating rate of 5°C $min^{-1}$.

### *Formation of δ-Phase Zn Compounds*

A $\delta$-phase Zn compound was easily obtained from other $\delta$-phase compounds such as a vanadyl intercalate $(VO)_{0.1}V_2O_5 \cdot nH_2O$ or potassium intercalate $K_{0.3}V_2O_5 \cdot nH_2O$ by ion-exchange treatment of soaking in a $ZnCl_2$ solution. This $\delta$-phase Zn compound was formulated by $\delta$-$Zn_{0.16}V_2O_5 \cdot nH_2O$ and found to exhibit reversible transitions between the phases with different layer spacings and degrees of hydration: 14.15 Å in wet (14.2-Å phase) 13.48 Å ($n \approx 2.2$) at RT (13.5-Å phase), 10.43 Å ($n \approx 1.0$) at 70°C (10.4-Å phase), and 9.31 Å ($n = 0$) at 180°C (9.3-Å phase). The same $\delta$-phase Zn compound exhibiting the 13.5-Å phase at RT was directly synthesized by the hydrothermal treatment of $VOSO_4$-$ZnSO_4$ mixed solutions at 220 to 280°C. The present hydrothermal system of $ZnCl_2$ $VO(OH)_2$ also produced a $\delta$-phase compound when reaction temperatures below 250°C were employed. This $\delta$ phase, which exhibited the 10.4-Å phase at RT instead of the 13.5-Å phase, was found to have higher Zn content as formulated by $\delta$-$Zn_{0.25}V_2O_5 \cdot nH_2O$ ($n \approx 1$). The $\delta$-phase Zn compounds may be compared with $\sigma$-phase analogues; the 10.4-Å $\delta$ phase corresponds to the hydrated 10.75-Å $\sigma$ phase and the anhydrous 9.3-Å $\delta$ phase to the anhydrous 8.98-Å $\sigma$ phase. It is noted that a difference between $\delta$ and $\sigma$ phase Zn compounds was also found in the ion-exchange activity that $\delta$ phase showed high ion-exchange activity while $\sigma$ phase showed no or little activity.

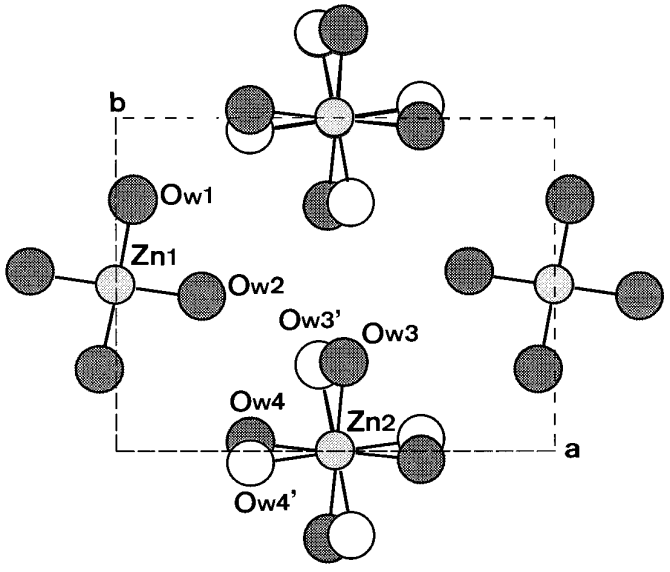


**FIG. 6.** Positional shifts of Ow3 and Ow4 to Ow3′ and Ow4′, respectively, to meet the $P2_1/a$ symmetry. Ow3′ and Ow4′ are obtained from Ow1 and Ow2, respectively, by the translation $(x + 1/2, 1/2 - y, z)$.

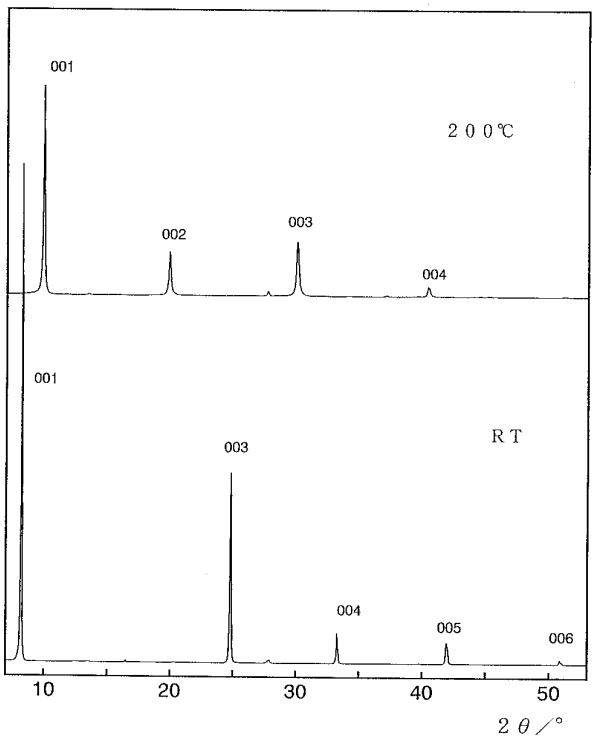


**FIG. 8.** Powder X-ray diffraction patterns for $\sigma$-$Zn_{0.25}V_2O_5 \cdot H_2O$ taken at RT (bottom) and 200°C (top).

## CONCLUDING REMARKS

A new layered phase of vanadium bronze designated as $\sigma$-$Zn_{0.25}V_2O_5 \cdot H_2O$ has been hydrothermally synthesized. A single-crystal study revealed a novel structure of a double-sheet-type $V_2O_5$ layer as well as interstitial sites of Zn atom and water molecule. The present study adds a new member to the family of vanadium bronzes having $V_2O_5$ layers. This new member appears to be related to the existing member of $\delta$ phase in terms of a double-sheet-type structure. The structure of $\sigma$ phase is featured by $VO_4$ tetrahedra coexisting with $VO_6$ and $VO_5$ polyhedra while that of $\delta$ phase is made up of $VO_6$ octahedra. Interstitial Zn atom is octahedrally coordinated by two apical oxygens of $VO_4$ tetrahedra on opposite sides and by four water molecules in a midplane. In the anhydrous phase this coordination must be drastically changed to contract the layer spacing by 1.83 Å. Production of isomorphous $\sigma$ phases has been observed for other divalent $M$ ions such as $M$ = Mg, Mn, Ni, and Co by our preliminary work, and the details will be reported elsewhere. It seems that $\sigma$ phase is formed with divalent metal ions while $\delta$ phase is formed with both mono- and divalent cations.

## ACKNOWLEDGMENTS

We are grateful to Professor S. Sasaki of Tokyo Institute of Technology for preparing and revising the computer programs. The present work is supported by Grant-in-Aid for Scientific Research from the Ministry of Education, Science, Sports and Culture of Japan. The drawings of crystal structures were produced with ATOMS by Shape Software.

## REFERENCES

1. P. Hagenmuller, *Prog. Solid State Chem.* **5,** 71 (1971).
2. K. Waltersson, "Chem. Commun. Univ. Stockholm No. 7" (1976).
3. H. G. Bachmann, F. R. Ahmed, and W. H. Barnes, *Z. Kristallogr.* **115,** 110 (1961).
4. F. Théobald, R. Cabara, and J. Bernard, *J. Solid State Chem.* **17,** 431 (1976).
5. T. Yao, Y. Oka, and N. Yamamoto, *Mater. Res. Bull.* **27,** 669 (1992).
6. P. Hagenmuller, J. Galy, M. Pouchard, and A. Cassalot, *Mater. Res., Bull.* **1,** 45 (1966).
7. P. Hagenmuller, J. Galy, M. Pouchard, and A. Cassalot, *Mater. Res., Bull.* **1,** 95 (1966).
8. J. Galy, A. Cassalot, M. Pouchard, and P. Hagenmuller, *C. R. Acad. Sci.* **262,** 1055 (1966).
9. S. Andersson, *Acta Chem. Scand.* **19,** 1371 (1965).
10. J. Galy, *J. Solid State Chem.* **100,** 229 (1992).
11. T. Yao, Y. Oka, and N. Yamamoto, *J. Mater. Chem.* **2,** 331 (1992).
12. Y. Oka, T. Yao, and N. Yamamoto, *J. Mater. Chem.* **5,** 1423 (1995).
13. T. Yao, Y. Oka, and N. Yamamoto, *J. Mater. Chem.* **2,** 337 (1992).
14. J. Galy, D. Lavaud, A. Cassarot, and P. Hagenmuller, *J. Solid State Chem.* **2,** 531 (1970).
15. J. Galy, J. Darriet, and P. Hagenmuller, *Rev. Chim. Miner.* **8,** 509 (1971).
16. S. Sasaki, private communication.
17. S. Sasaki, KEK Internal Report, Vol. 3, National Laboratory of High Energy Physics, Tukuba, Japan, 1987.
18. "International Tables for X-ray Crystallography IV." Kynoch Press, Birmingham, UK, 1974.
19. TEXSAN: Crystal Structure Analysis Package, Molecular Structure Corp., The Woodland, TX, 1985 & 1992.